Aerodynamic performance enhancement of a Savonius wind turbine using an axisymmetric deflector

Hady Aboujaoude, Fabien Beaumont, Sébastien Murer, Guillaume Polidori, Fabien Bogard

Journal of Wind Engineering and Industrial Aerodynamics

Aerodynamic performance enhancement of a Savonius wind turbine using an axisymmetric deflector

Hady ABOUJAOUDE[1], Fabien BEAUMONT[1], Sébastien MURER[1], Guillaume POLIDORI[1], Fabien BOGARD[1,2*]

[1]MATIM, Université de Reims Champagne-Ardenne, Reims, France
[2]Pôle de Recherche Châlonnais, Université de Reims Champagne-Ardenne, Châlons en Champagne, France

* **Corresponding author**: Fabien BOGARD, fabien.bogard@univ-reims.fr

Abstract

The installation of wind turbines in urban sites requires consideration of the wind characteristics affecting the energy production (turbulence, environment roughness due to the surrounding buildings...), the self-starting capability and the type, hence the performance, of the wind turbine. In this paper, a three-dimensional CFD analysis of an aerodynamic Savonius wind turbine is performed under steady wind conditions. The inclusion of a deflector was also investigated, and the performance compared to the initial design.

Results of the 3D analysis showed that an optimized axisymmetric deflector improves the power coefficient in all wind directions and over the entire operating range of the turbine. The deflector also increased the average starting torque by 30%, thus extending the operating range of the turbine with respect to the wind speed.

Keywords: Vertical axis wind turbine, transient three-dimensional simulation, power coefficient, Savonius rotor, aerodynamics

1. Introduction

Wind energy is a powerful, efficient, and sustainable source of electricity. Yet urban wind turbines represent a negligible part of the total number of wind turbines (less than 10,000 in France). They are part of the small wind category (between 1 and 36 kW) according to the French (ADEME, 2015) and British (IRENA, 2015) segmentations, and are grouped under the name "small wind" in the USA (Clausen et Wood, 2000).

Until the late 2010s, interest in Urban Wind Turbines (UWT) was modest compared to other categories. In spite of the recently implemented optimized systems, UWTs display average efficiency, are not necessarily cheap and pose reliability problems. For all these reasons, the interest towards these systems, and the associated research, remains limited, although they constitute an additional energy source and can thus contribute to the energy autonomy of individuals and small companies. The main scientific hurdle is to improve their efficiency by considering both the urban environment and the specifics of urban winds, i.e. turbulence and irregularities. The present study focuses on aerodynamic optimization of a Savonius wind turbine, in view of their particular characteristics such as self-starting capability and structural stability (Kedare and Date, 1999; Wenehenubun et al., 2015).

Fig. 1. Examples of Savonius wind turbines.

The Savonius rotor consists of two vertical half-cylinders rotating around a vertical axis, but whose planar ends are offset from each other. Different shapes exist, as seen in Fig. 1.
The extensive bibliographic references on this topic help understand the dynamic behavior of this type of wind turbine; the difference in drag forces between the convex and concave blades produces a mechanical torque which ensures the rotation of turbine around its axis, as depicted in Fig. 2. However, the wide range of turbine geometries, wind speeds and experimental conditions makes it difficult to compare wind turbines and select the optimal one.

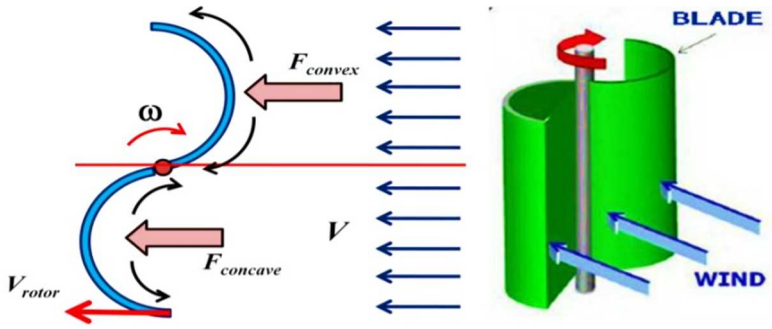

Fig. 2. Operating principle of a Savonius wind turbine (Mohamed, 2013).

The results of numerical simulations performed on new Savonius wind turbine designs (static or dynamic) are usually presented by comparing the developed torque, the torque coefficient C_T (Eq.1) and the power coefficient C_P (Eq.2), relative to the rotational speed (for the dynamic models) (Mauro et al., 2019; Meziane et al., 2020; Zakaria et al., 2020; Marinic et al., 2019).

$$C_T = \frac{T}{0.5\,\rho\,V_\infty^2\,A\,R} \quad (1)$$

$$C_P = \frac{T\,\omega}{0.5\,\rho\,V_\infty^3\,A} \quad (2)$$

T is the torque developed around the axis of the wind turbine, ω is the rotational speed of the wind turbine, ρ is the air density, V_∞ is the free airstream velocity and A is the swept area.
Fig. 3 summarizes the orders of magnitude for C_P coefficients to be used depending on tip-speed ratio λ (Eq. 3), which is defined as follows:

$$\lambda = \frac{R*\omega}{V_\infty} \quad (3)$$

with R the radius of the turbine.

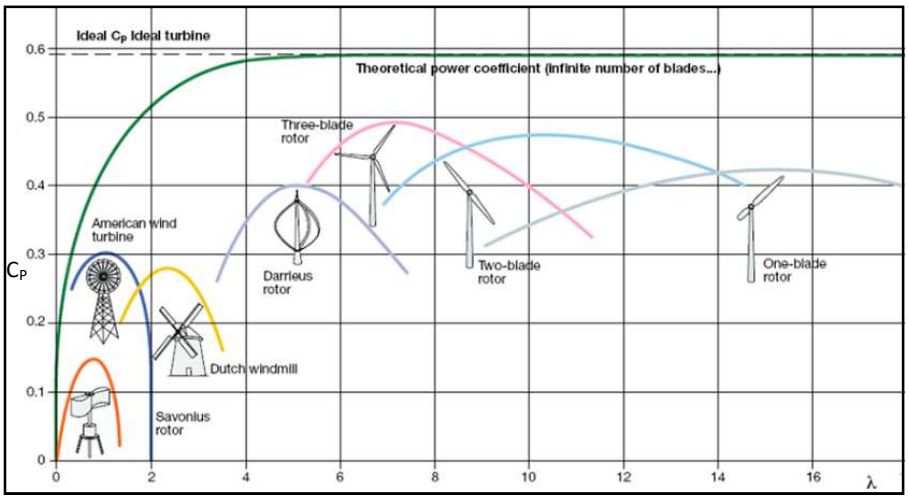

Fig.3. Power coefficient C_P for different wind turbine designs vs. tip-speed ratio λ (Alabdali et al., 2020).

It is worth noting that Savonius wind turbines are meant to be used in the lowest wind velocity conditions. Together with its high starting torque, which translates into the possibility of starting without back-up power, makes them perfectly suitable for urban areas where wind speed is naturally lower than in rural areas.

However, the Savonius rotor ranks low in terms of power coefficient value, but this may be of interest because the low induced tip-speed ratio translates into low acoustic nuisance (Mojica et al., 2019). This wind turbine, similarly to the Darrieus for that matter, also has the ability to take advantage of wind in all directions, without the need for a detection and control system which are mandatory for horizontal axis models. The Savonius wind turbine is also structurally superior to others and is therefore able to better resist the turbulent winds encountered in urban areas.

Several researchers and engineers have proposed innovative systems to increase the airflow to the turbine. Although the Betz limit caps the maximum fraction of power that a wind turbine can extract from the available wind at 59.3%, this limit may be extended by using an air converging system. Botempo et al. (2020) studied the development of an ideal air deflector upstream of a wind turbine and proved that the Betz limit can be exceeded.

Indeed, the power extracted from the wind is directly related to the velocity difference upstream and downstream of the wind turbine. Any increase in upstream wind velocity will increase the efficiency of the system: to this end, deflectors concentrate the mass flow of the wind toward the working area of the turbine, which increases the incoming wind speed. As seen in Fig. 4, several deflector designs have been developed over the last 40 years. Alexander et al. (1978) studied the combination of a flat and circular shield (Fig. 4a), and calculated C_{Pmax}=0.243. Morcos et al. (1981) used a flat-shaped baffle plate facing the wind turbine (Fig. 4b) and reported C_{Pmax}=0.34. Ogawa et al. (1986) used a V-shaped baffle plate (Fig. 4c) which resulted in a C_{Pmax} value of 0.212. Shaughnessy et al. (1992) investigated another type of V-shaped wind concentrator (Fig. 4d) which increases power by nearly 19.7% compared to a standard rotor with no deflector.

Circular deflectors (Fig. 4e) have also been investigated to decrease the wind pressure exerted on the convex blade (Yonghai et al., 2009). The use of concentration deflectors (Fig. 4f) upstream of the rotor minimizes the flow on the returning blade to reduce the negative torque (Burçin et al., 2010). One more paper discusses the integration of an obstacle shield (Fig. 4g) to lower the negative torque, which improves the rotor performance by up to 30% (Mohammed et al., 2010). Golecha et al. (2011) used a deflector plate (Fig. 4h) upstream of the advancing blade and achieved a 50% increase in performance over the semi-circular bladed rotor. Roy et al. (2014) used wind deflectors at the inlet (Fig. 4i) and obtained C_{Pmax}=0.32. Guide vanes (Fig. 4j) also improve the rotor performance (El-Askary et al., 2015). Finally, a conveyor-deflector curtain (Fig. 4k) placed in a conventional Savonius rotor increased C_P up to 0.30 (Tartuferi et al., 2015).

Authors	Deflector designs
(a) Alexander et al. (1978)	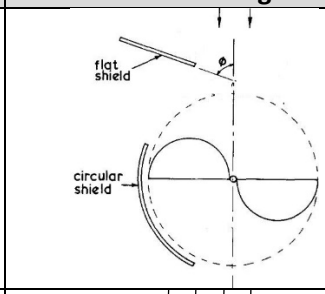
(b) Morcos et al. (1981)	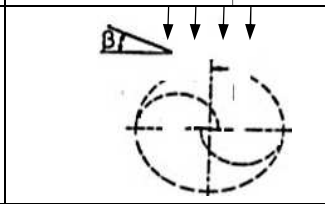
(c) Shaughnessy et al. (1992)	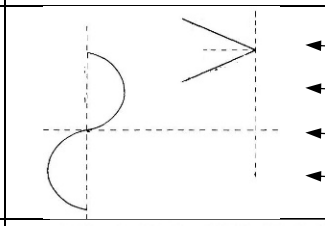
(d) Ogawa et al. (1986)	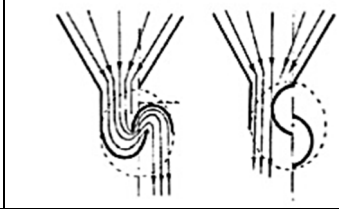
(e) Yonghai et al. (2009)	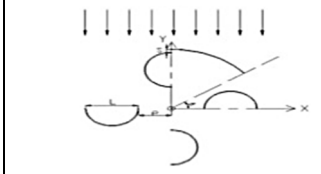
(f) Burçin et al. (2010)	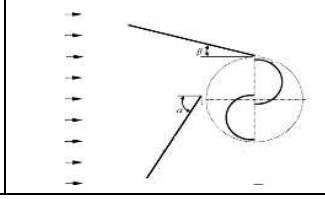

Authors	Deflector designs
(g) Mohammed et al. (2010)	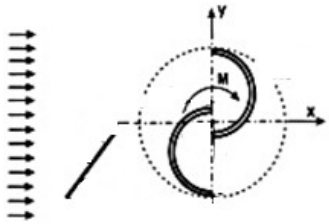
(h) Golecha et al. (2011)	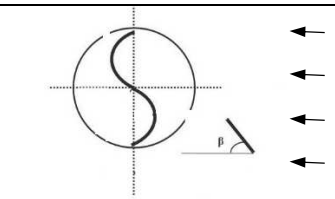
(i) Roy et al. (2014)	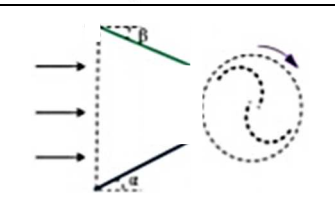
(j) El-Askary et al. (2015)	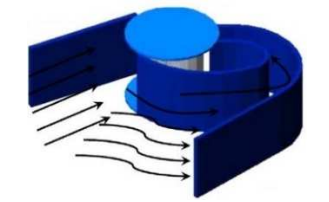
(k) Tartuferi et al. (2015)	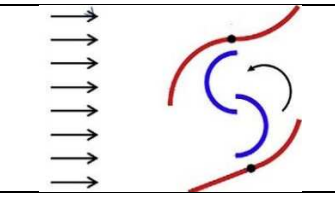

Fig. 4. Different convergent designs for Savonius wind turbines.

The main drawback of these systems is operating mode, which increases the turbine efficiency for one wind direction only.

Moreover, numerical studies focusing on the performance of deflectors are usually performed in 2D, without considering the wake effect, the height/diameter ratio of the wind turbine or the presence of end plates. It can be assumed that their results may be optimistic compared to experimental data.

Some of these deflectors require a steering mechanism for proper alignment with the wind direction, but these additional devices consume energy, add complexity and weak points in the maintenance.

The objective of this study is therefore to propose a system able to concentrate the incoming airflow from all directions while remaining simple in design, with no energy-consuming steering mechanism to reduce future maintenance interventions.

The aerodynamic optimization of the wind turbine requires the addition of a single part, with simple design and manufacturing, namely an axisymmetric deflector that requires no alignment in the wind direction. To the best of the authors' knowledge, such device has never been studied before in the

literature. For this purpose, a Savonius wind turbine has been parameterized, and a 3D numerical optimization has been performed to define the optimal dimensional characteristics of the deflector. In a second step, the numerical results have been compared with experimental data from the literature for validation purposes.
Results obtained from the 3D numerical model will help define potential improvements in the turbine performance, by adding an optimal deflector in an urban operating environment.

2. Methodology

2.1. Geometry of the Savonius wind turbine model

The main geometric parameters impacting the performance of the Savonius rotor are summarized in Fig. 5 and are defined as follows:

- The blades of a Savonius wind turbine are typically between 1 and 3 in number. As mentioned by previous studies (Ross et al., 2011; Akwa et al., 2012), we selected a 2-blade system which features the best performance and power coefficient.
- The ratio of turbine height to turbine diameter called Aspect Ratio A_R = H/D. Sobczak et al. (2018) note that an A_R ratio between 1.0 and 2.0 is a good compromise between performance and compactness. We selected A_R = 1.66, defined by height H=1.5m and diameter D= 0.9 m.
- The presence or absence of end plates on which the blades rest to channel the incident flow. Saha et al. (2008) recommend an optimal ratio of 1.1 between the plates and rotor diameters.
- The dimensionless gap width defined by ratio e/d. According to Fujisawa et al. (1991), turbine efficiency is optimal for a value of 0.15. Blackwell et al. (1977) propose a range from 0.1 to 0.15, while Menet (2004) advises a value 0.242 and Akwa et al. (2012) 0.15. In view of these recommendations, we opt for an overlap value of 0.15.

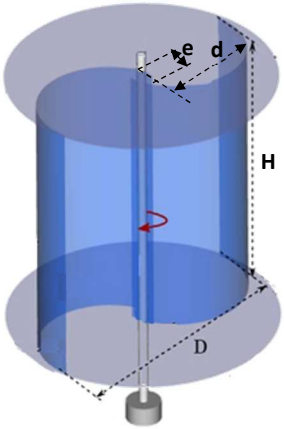

Fig. 5. Geometric parameters of the Savonius wind turbine (Roy et al., 2018).

2.2. Key features of the deflector

As shown in Fig. 6, the convergent has a simple, axisymmetric shape. The profile consists of a truncated cone whose dimensions will be defined by a geometric optimization on the following parameters: A is the gap between the convergent and the turbine; B, the large diameter of the truncated cone; C, the small diameter of the truncated cone and D the height of the truncated cone. The deflector truncated cones are non-rotating fixed. Although the mounting system of the deflectors is not represented in Fig. 6, it is thought to be completely dissociated and independent from the turbine structure.

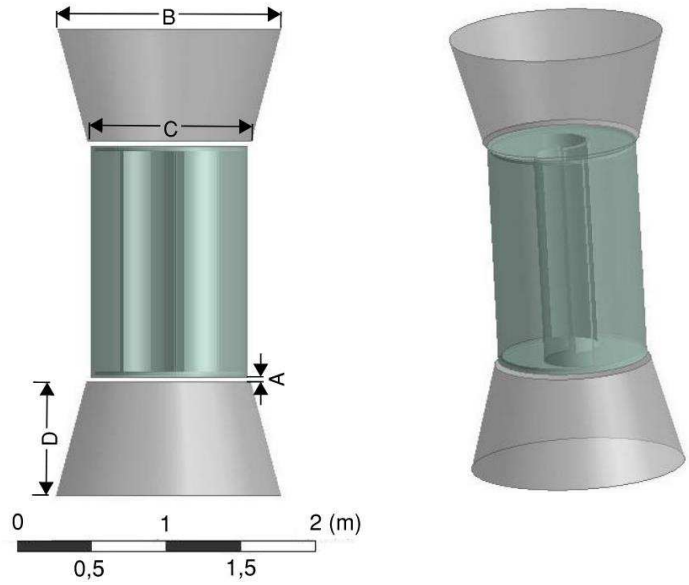

Fig. 6. Geometry of the deflector used.

The optimization of these dimensional parameters aims at maximizing the static torque developed around the turbine axis. 3D optimization is achieved using the ANSYS© response surface tool. After setting the geometric constraints of our input parameters A, B, C and D and the target output parameter, a sensitivity study is proposed in the form of a response surface with respect to the most influential parameters. After several iterations, the optimal dimensions obtained for the deflector are: A = 5 cm; B = 150 cm; C = 105 cm and D = 75 cm.

2.3. Geometric parameters of the numerical model

The present study is based on a dynamic three-dimensional CFD simulation. The geometry of the urban wind turbine was created using ANSYS DesignModeler© software. The use of a sliding mesh to simulate the rotation of the wind turbine around its axis required the creation of 2 domains: one stationary and one rotating. The dimensions of the computational domain shown in Fig. 7 were chosen according to the recommendations of El-Askary et al. (2015). Computations and post-processing were performed using FLUENT© 2020 R2. Several rotational speeds are imposed to the rotating subdomain to model the aerodynamic performance of the wind turbine over the entire operating range.

Boundary conditions involve a no-slip condition on the fixed walls of the stationary domain, as well as on the deflector and wind turbine. A constant velocity of 7 m/s with a turbulence intensity of 5% is imposed at the inlet of the computational domain and a pressure-outlet condition (constant atmospheric pressure) is imposed at the outlet.

The velocity used for the calculation of power coefficient C_P is rectified according to (Eq.4; Eq.5) to account for the flow concentration induced by the external domain walls:

$$V = V_\infty(1 + \varepsilon_t) \quad (4)$$

$$\varepsilon_t = \frac{1}{4}\frac{A_t}{A_{wt}} \quad (5)$$

with A_t the frontal section of the wind turbine and A_{wt} the fixed section of the domain (Ross et al., 2011; Jeong et al., 2018).

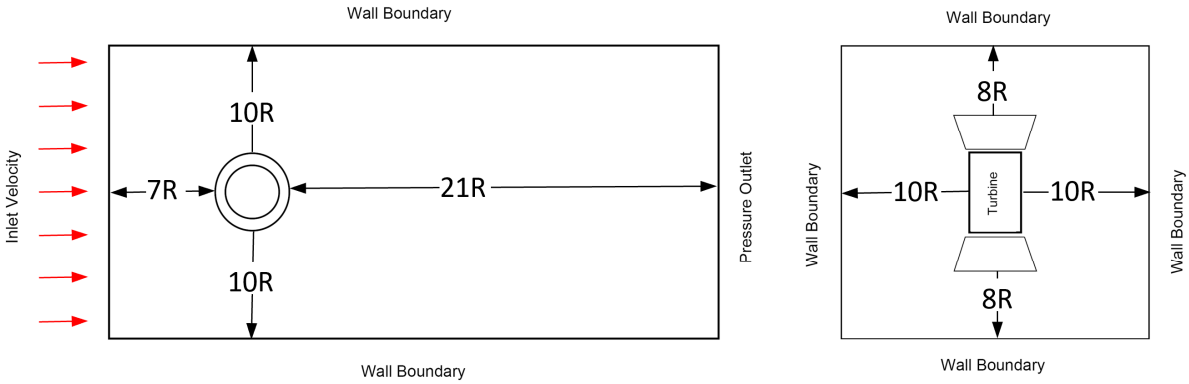

Fig. 7. Domain dimensions and boundary conditions.

2.3.1. Stationary and sliding meshes

Simulation of a system involving a rotating part is a challenge that requires the use of the sliding meshing method (Marmutova 2016), as the rotating motion of the rotor requires a separate region with different meshing requirements (deflectors are fixed). The stationary subdomain is obtained by extracting the rotating part and the designed deflector from the initial computational domain. Then the rotating subdomain is modeled and added as a separate cylinder, as seen in Fig. 8. An optimal interface between the two subdomains is achieved using the shared topology method at the geometry level, which the meshing is developed upon.

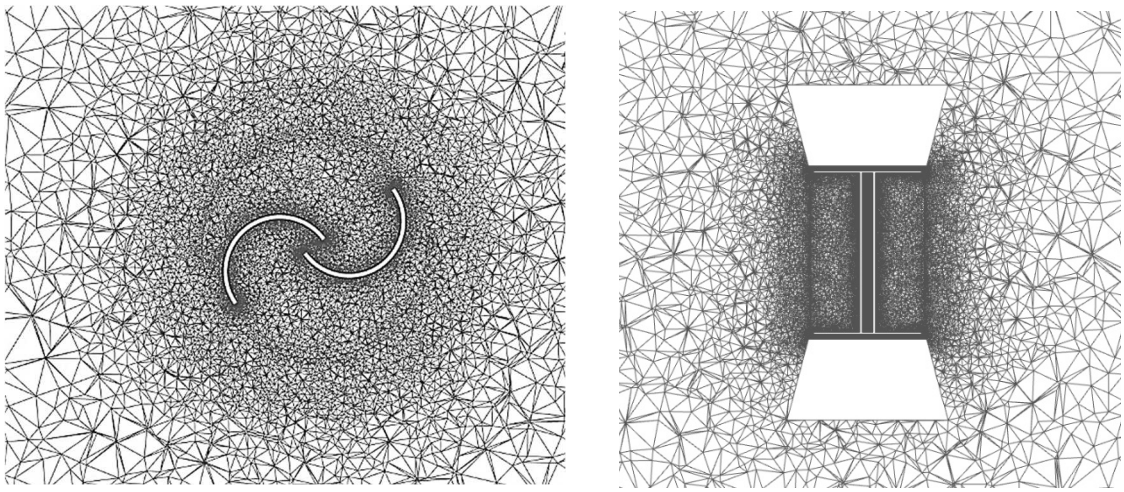

Fig. 8. Details of the stationary and sliding meshes.

An unstructured mesh was generated using Ansys meshing software and consists of 4.5 million tetrahedral elements Fig. 8. A mesh sensitivity analysis was performed on a 4.5, 6 and 7 million tetrahedral element meshes and showed no significant improvement in the accuracy of the output torque. Downstream of the rotor, the mesh was refined to capture wake vortices. In addition, an inflation mesh consisting of 18 layers of prismatic elements around the blades was created around the airfoil to reach appropriate y+ values. The dimensionless height of the first mesh node adjacent to wall y+ has a major impact on the simulation results. Indeed, the torque produced around the axis of the wind turbine imposes a fine resolution of the viscous sublayer, hence the need for a y+ value below 5 on the blades. This optimized mesh made it possible to achieve an average value of y+ of 1.8 on the turbine surface.

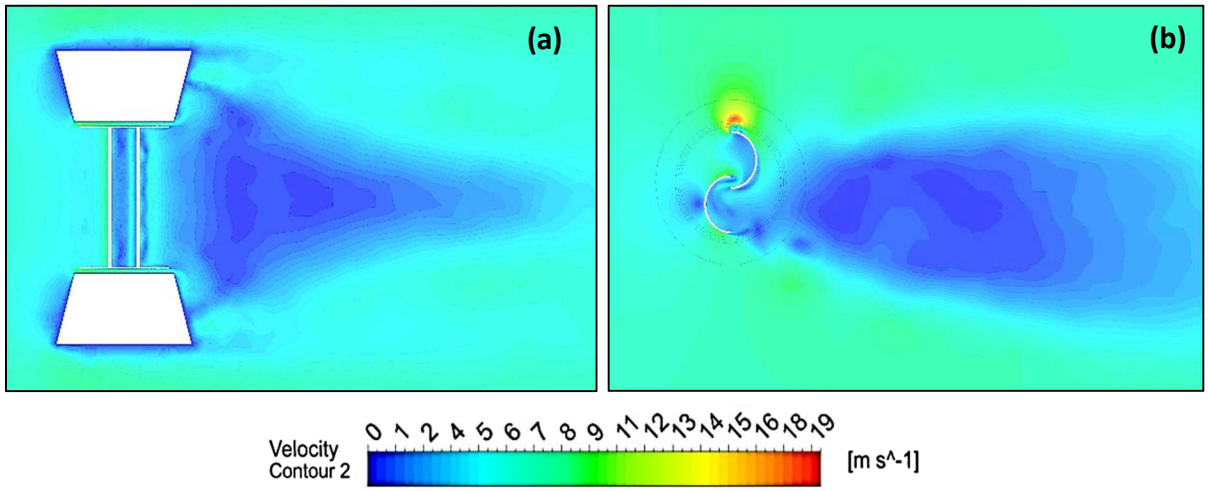

Fig. 9. Visualization of the velocity continuity between the 2 meshed subdomains. **(a)** horizontal velocity contour at z = 0, **(b)** vertical velocity contour at y = 0.

2.3.2. Turbulence model

The most widely used turbulence model to account for the aerodynamic behavior of 3D wind turbines is Kω–SST (Rezaieha et al., 2019; Ghazalla et al., 2019; Alom et al., 2021). Several other models are also implemented like TSST (Saheen et al., 2015) or Realizable K-ε (Mohammed et Thevenin, 2010; Kumar et al., 2017). Numerical comparisons with experimental data from Blackwell et al. (1977) showed that all these numerical models underestimate the experimental results, which is consistent with studies by Ferrari et al. (2017) and Mohammed et al. (2010). It was also found that the Kω–SST model is the most appropriate for our simulations, as seen in Fig. 10. This model was therefore selected.

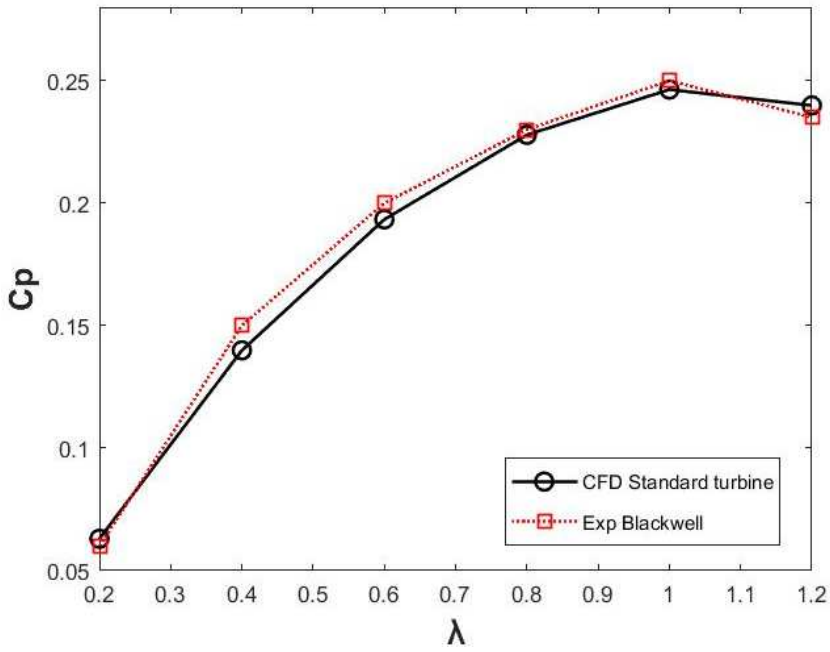

Fig. 10. Comparison of power coefficient C_P between experimental data from Blackwell et al. (1977) and the dynamic, Kω–SST-based simulation model with rotating mesh vs. velocity coefficient λ.

Scientific works about wind turbines generally rely on power coefficient C_P for both evaluation and comparison purposes, since it quantifies the performance of the turbine over the entire

operating spectrum. As such, this parameter constitutes a reliable measure of the capacity of the turbine to collect energy from the wind.

2.3.3. Simulation settings

To evaluate the wind turbine performance over the whole operating range, six values of tip-speed ratio λ were simulated (0.2 to 1.2, step 0.2). The values of λ, corresponding angular velocities and time steps used for each calculation are summarized in Tab.1.
The time step is set to a value corresponding to the time needed for the turbine to perform a 0.5° and -1° rotation for each value of λ. Such precaution avoids divergences in CFD computations (Marmutova 2016).

λ	0.2	0.4	0.6	0.8	1	1.2
Angular velocity (rd.s^{-1})	2.8	5.6	8.4	11.2	14	16.8
Time Step (s)	0.005	0.002	0.0015	0.0012	0.001	0.0008

Table 1 Simulation settings.

Monitoring the torque developed around the wind turbine axis makes it possible to assess its aerodynamic performance. Indeed, in the case of an "ideal" rotating turbine (i.e. without friction), the value of torque would be zero for a constant, imposed wind velocity in a stationary regime. Therefore, it is sufficient to evaluate and compare, under identical conditions, the values of torque with and without a deflector to conclude on the induced impact on the intrinsic performance of the wind turbine. Practically, an increase in performance will translate in the resulted torque as well as the power coefficient C_P.

3. Results

C_T and C_P coefficients are key indicators of the wind turbine performance and are widely used in the literature as a basis for comparison between numerical and experimental results. As shown in Eq.1 and Eq.2, for a constant wind velocity and an imposed angular velocity, calculating the torque delivered around the axis of the wind turbine is the only way of obtaining power coefficient C_P of the different wind turbines. As far as numerical simulations are concerned, only this physical parameter is able to predict the performance of the wind turbine proposed in this study. The
Torques delivered by conventional (without deflector) and updated (with deflector) wind turbine are plotted in Fig. 11, for all values of λ summarized in Tab. 1. It is noted that the torque representations shown in Fig. 11 were plotted after 5 complete revolutions to ensure stabilization of the results.
Furthermore, the pressure contours of these 2 wind turbines are displayed in Fig. 12 for two different angular positions in which torque is negative. Fig. 13 displays the pressure contours along with the velocity streamlines flowing through the wind turbine. Finally, Fig. 14 summarizes the performance of the wind turbines by evaluating the delivered torque versus angular velocity in RPM (Fig. 14a), and power coefficient C_P versus velocity coefficient λ (Fig. 14b).

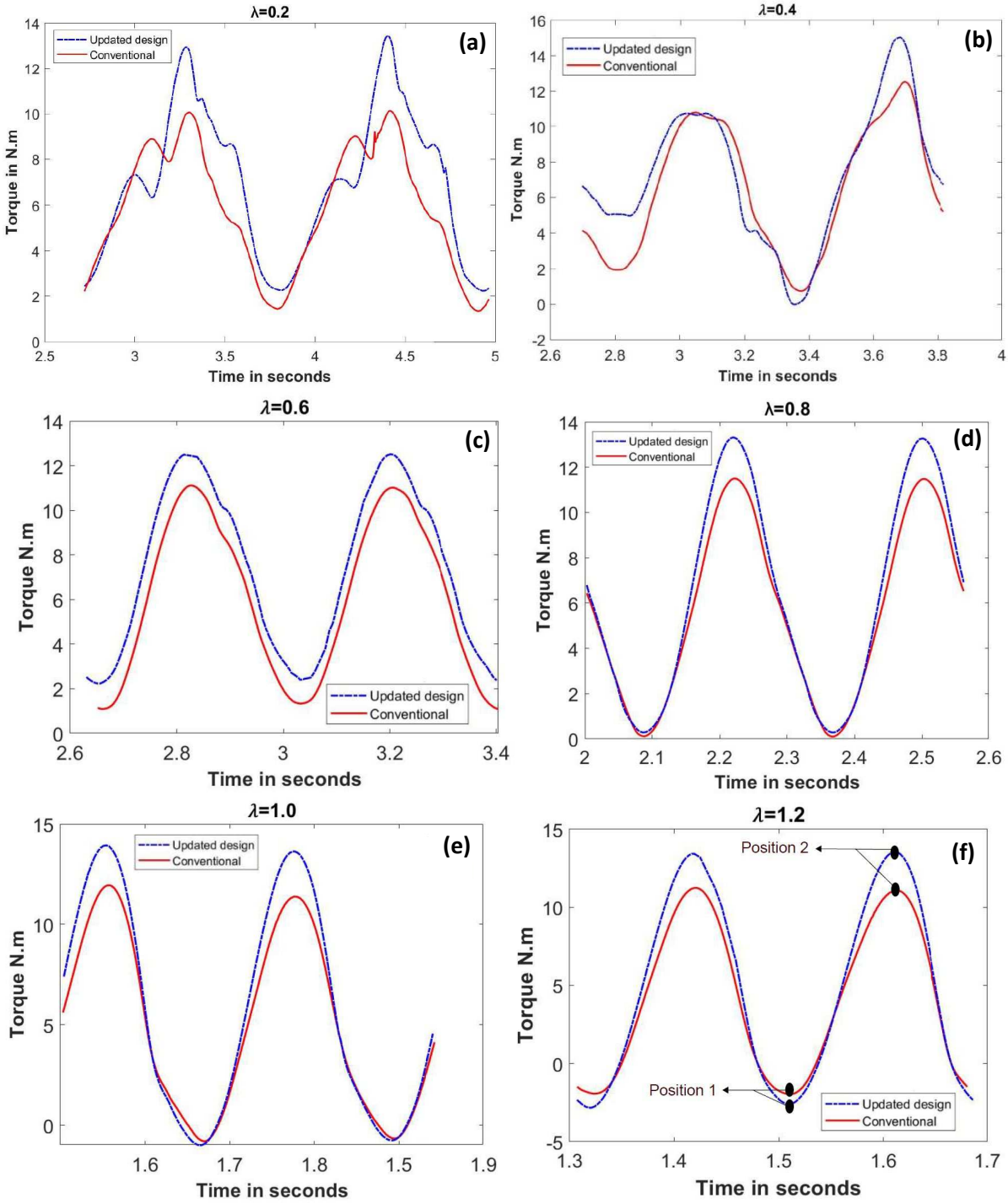

Fig. 11. Instantaneous torque around the axis of the wind turbine, with (dotted) and without (solid) deflector for different values of λ.

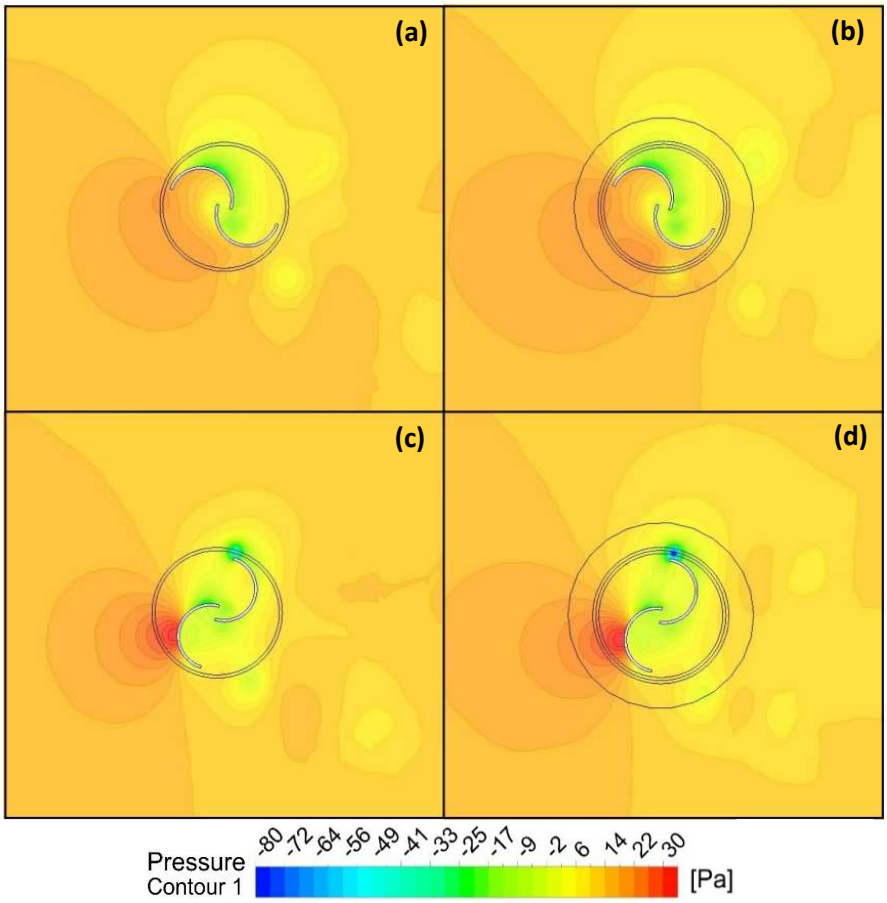

Fig. 12. Pressure contours in the median plane with and without convergent for an angular velocity of 160 RPM at different angular positions noted in Fig. 11f. **(a)** conventional wind turbine - angular position 1, **(b)** wind turbine with deflector - angular position 1, **(c)** conventional wind turbine - angular position 2, **(d)** wind turbine with deflector - angular position 2.

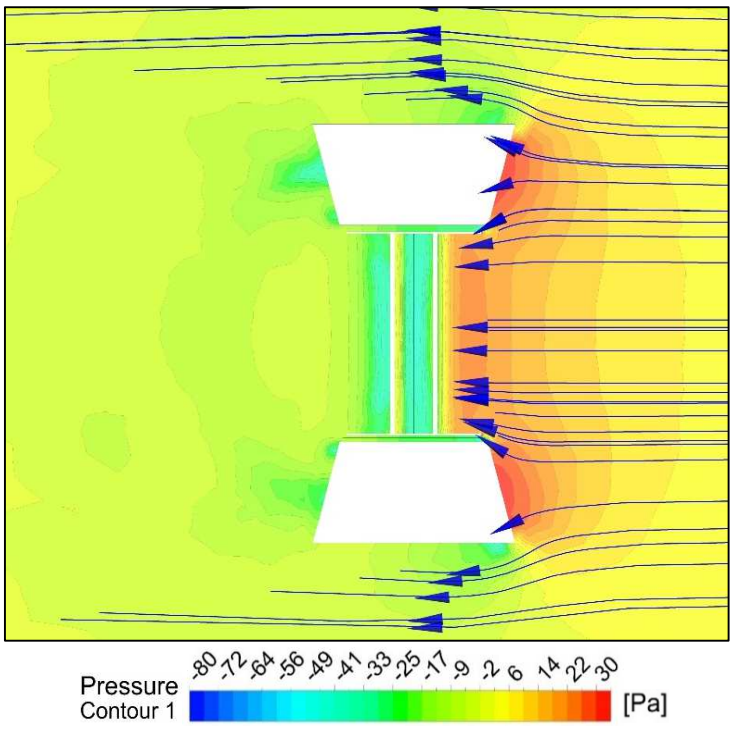

Fig. 13. Pressure contours in the median plane with velocity streamlines.

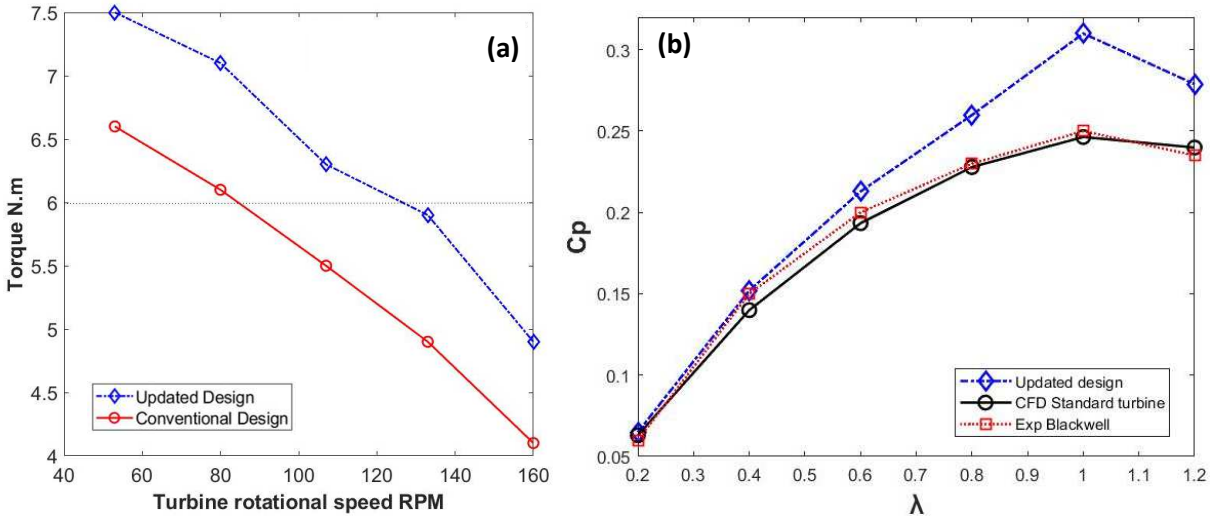

Fig. 14. (a) Delivered torque vs. angular velocity; **(b)** Comparison of C_P between experimental data from Blackwell et al. (1977), numerical results of the conventional wind turbine and of the wind turbine with convergent.

4. Discussion

Fig. 11 shows that the evolution of torque value is periodic, with fluctuations around a mean value. The performance of the wind turbine depends on the angular position of the rotor, and reach higher values for given angular positions. By calculating the average torque for different tip speed ratios λ, the power coefficients C_P of different wind turbines can be obtained. Besides, knowledge of these fluctuations is valuable in the structural design of wind turbines.

Under a wind speed of 7 $m.s^{-1}$, the average torque of both wind turbines decreases as λ increases, which is expected since relative wind velocity with respect to the rotating blades decreases with the increase of the angular velocity. Fig. 11 shows similar curves for the two types of turbines, except that a noticeable offset from the ordinate axis is observed. The average torques vs. angular velocity are shown in Fig. 14a. Clearly, the wind turbine with axisymmetric deflector delivers higher torques compared to the conventional wind turbine under the same conditions and can be considered as significantly more efficient. A similar conclusion may be drawn by analyzing Fig. 14b, with higher values of coefficient C_P for the new design. It is worth noting that the C_P computation based on the Eq. 2 used the same swept area A for the two proposed turbines, which is the only rotating in both configurations.

The velocity streamlines plotted in Fig. 13 reflect the working mechanism of the proposed deflector. Naturally, the truncated cones redirect the airflow to the rotor which increases the mass flow rate of air moving through the turbine. Pressure upstream the rotor is increased, as reflected in Fig. 13.

Torque fluctuations are much more pronounced at low speeds, and the curves become smoother and more sinusoidal at high angular velocities. Such result does not stem from numerical errors, since all computations are carried out using a time step that corresponds to a rotation of 0.5° to -1°.

To study the aerodynamics at angular position 1 (negative torque, constant wind speed, angular velocity 160 RPM, see Fig. 11f), the pressure contours have been plotted in Fig. 12c and Fig. 12d. The difference between the upstream and downstream pressure around each blade defines the drag force. Quite expectedly, the drag force on the driven blade is much larger than that on the driving blade. Fig. 12c.d shows a more pronounced pressure contrast (red upstream / blue downstream) on the driven blade compared to the driving paddle (green upstream / green downstream). The driven blade therefore prevails, and the resulting torque is negative which induces braking of the wind turbine at 1.5 s when the angular velocity of the turbine is at 160 RPM. It is also worth mentioning that the average non-instantaneous torque has a positive value of 4.9 Nm (with convergent) and 4.1 Nm for a conventional Savonius wind turbine.

Regarding angular position 2 (positive torque, constant wind speed, angular velocity 160 RPM, see Fig. 12f), the pressure contours have been plotted in Fig. 12a and Fig. 12b. The pressure contrast is more pronounced on the driving blade, leading to positive torque and acceleration of the turbine at 1.62 s when the turbine is rotating at 160 RPM.

Considering a constant torque value of 6 Nm, the two turbines display different angular velocities. Indeed, as shown in Fig. 14a, the conventional wind turbine rotates at 84 RPM, while the convergent one can rotate at 126 RPM, i.e. an increase of 50% in angular velocity resulting in significant gain in the power coefficient (see Eq.2).

Finally, the dynamic 3D simulation highlights that the wind turbine with optimized deflector increases the Savonius performance coefficient by 25% over the entire speed range (including start-up), with C_{Pmax}=0.31, recorded for a velocity coefficient λ=1.0 (see Fig. 14b).

Table 2 presents literature results of studies conducted on deflectors, all with static unidirectional orientation, i.e. concentration of wind coming from a predominant direction. These deflectors have a negative impact on all other directions, unless a yaw mechanism is added. However, as mentioned earlier, higher energy consumption and more complex design and maintenance should be considered. Considering that urban winds are turbulent in both amplitude and direction, axisymmetric deflectors will perform better and collect more energy. Yet systems featuring values of C_{Pmax} greater than 0.31 are derived from experiments carried out in wind tunnels or 2D CFD simulations, which are known to be more "optimistic" than 3D CFD simulations, as indicated by Marinic et al. (2020) and Ferrari et al. (2017).

Authors	Design	Reported C_{Pmax}	Study	Wind concentrator
El-Askary et al., 2015	Curtain design	>0.5	2D CFD	Unidirectional
Burçin et al., 2010	Curtain design	0.38	Wind tunnel	Unidirectional
Morcos et al., 1981	Flat plate shield	0.34	Wind tunnel	Unidirectional
Roy et al., 2013	V-shaped deflector	0.32	Wind tunnel	Unidirectional
Present work	***Axisymmetric deflector***	***0.31***	***3D CFD***	***Axisymmetric multidirectional***
Tartuferi et al., 2015	Curtain design	0.3	2D CFD	Self-rotating
Yonghai et al., 2009	Deflector plate	0.28*	2D CFD	Unidirectional
Golecha et al., 2011	Deflector plate	0.26	Wind tunnel	Unidirectional
Mohamed et al., 2010	Obstacle shielding	0.25	2D CFD	Unidirectional
Mohamed et Thevenin, 2010	Obstacle shielding with guide vane	0.25	2D CFD	Unidirectional
Alexander et Holownia, 1978	Flat plate shield	0.24	Wind tunnel	Unidirectional
Ogawa et Yoshida, 1986	Deflector plate	0.22*	Wind tunnel	Unidirectional
Ogawa et Yoshida, 1986	Deflector plate	0.21	Wind tunnel	Unidirectional
Shaughnessy et Probert, 1992	V-shaped deflector	<0.12*	Wind tunnel	Unidirectional

Table 2 C_{Pmax} reported in the literature for Savonius deflectors. The values of C_{Pmax} in studies marked with an asterisk* were extrapolated.

The deflector design is easy to manufacture and can be independent of the wind turbine design. It can be added to existing Savonius turbines at reasonable cost, or even be adapted to other types of axial wind turbines, such as Darrieus turbines which offer higher levels of performance.

5. Conclusion

In this work, a new type of deflector for the Savonius wind turbine is presented to improve its performance. This deflector is an axisymmetric truncated cone, designed and optimized by a numerical method. The main advantage of this shape is that it redirects the wind from all directions into the Savonius blades. Current devices which are unidirectional fully functional for only one wind direction unless they are equipped with a specific system of reorientation in the wind direction. The proposed solution has the advantage of being free of any risk of maladjustment or maintenance. It does not require any specific mechanism because the deflectors are immobile. Comparisons between experimental measurements from the literature and a numerical model with and without a deflector were performed. Three-dimensional simulations with the KSST turbulence model have demonstrated the potential of a wind turbine equipped with this deflector, as well as its advantages

over the solutions studied in the literature. This new deflector allows to reach a value of CPmax=0.31 and thus to increase the performance of the wind turbine by 25% in all wind configurations (intensity and direction) as well as at start-up, a key issue in the field of urban wind turbines.

Other works, both numerical and experimental, are in progress, and investigate the possible improvements of this deflector, or on its behavior in an urban environment (presence of obstacles or combination of several wind turbines and influence of the wakes, for example) as well as on its adaptation to a Darrieus-type wind turbine.

Acknowledgments

The authors wish to thank the Communauté d'Agglomération de Châlons en Champagne (France) and the Pôle de Recherche Châlonnais for their material support.

References

ADEME, 2015. Fiche technique du petit éolien, 11p.

Akwa J.V., Vielmo H.A., Petry A.P. 2012. A review on the performance of Savonius wind turbines. Renew. Sustai. Energy Rev. 16 (5), 3054-3064. https://doi.org/10.1016/j.rser.2012.02.056

Alabdali Q.A., Bajawi A.M., Fatani A.M., Nahhas A.M. 2020. Review of recent advances of wind Energy. Sustainable Energy 8(1), 12-19. https://doi.org/10.12691/rse-8-1-3

Alexander A., Holownia B. 1978. Wind tunnel tests on a savonius rotor. J. Industrial Aerodynamics, 3, 343-351. https://doi.org/10.1016/0167-6105(78)90037-5

Alom N., Saha U.K.,Dean A. 2021. In the quest of an appropriate turbulence model for analyzing the aerodynamics of a conventional Savonius (S-type) wind rotor. Journal of Renewable and Sustainable Energy. https://doi.org/10.1063/5.0034362

Blackwell B.F., Sheldahl R.E., Feltz L.V. 1977. Wind Tunnel Performance data for two and three bucket Savonius rotor. Sandia National Laboratories Report, SAND76-0l30

Bontempo R., Manna M. 2020. On the potential of the ideal diffuser augmented wind turbine: an investigation by means of a momentum theory approach and of a free-wake ring-vortex actuator disk model. Energy Conversion and Management 213:112794. https://doi.org/10.1016/j.enconman.2020.112794

Burçin D.A., Mehmet A. 2010. The use of a curtain design to increase the performance level of a Savonius wind rotors. Renewable Energy 35, 821-829. https://doi.org/10.1016/j.renene.2009.08.025

Clausen P.D., Wood D.H. 2000. Recent advances in small wind turbine technology. Wind engineering volume 24 N°3. https://doi.org/10.1260/0309524001495558

El-Askary W.A., Nasef M.H., Abdelhamid A.A., Gad H.E. 2015. Harvesting wind energy for improving performance of Savonius rotor. J Wind Eng. Ind. Aerodyn. 139:8–1. https://doi.org/10.1016/j.jweia.2015.01.003

Ferrari G., Federici D., Schito P., Inzoli F., Mereu R. 2017. CFD study of Savonius wind turbine: 3D model validation and parametric analysis. Renewable Energy 105:722-734. https://doi.org/10.1016/j.renene.2016.12.077

Fujisawa N. 1991. On the torque mechanism of Savonius rotors. J Wind Enginee. and Industrial Aerodynamics 40:277-292 . https://doi.org/10.1016/0167-6105(92)90380-S

Ghazalla R.A., Mohamed M.H., Hafiz A.A. 2019. Synergistic analysis of a Darrieus wind turbine using computational fluid dynamics. Energy 189:116214. https://doi.org/10.1016/j.energy.2019.116214

Golecha K., Eldho T.I., Prabhu S.V. 2011. Influence of the deflector plate on the performance of modified Savonius water turbine. Applied Energy 88, 3207-3217. https://doi.org/10.1016/j.apenergy.2011.03.025

IRENA. 2015. Quality Infrastructure for Renewable Energy Technologies Small Wind Turbines. ISBN : 978-92-95111-21-9.

Jeong H., Lee S., Kwon S.D., 2018. Blockage corrections for wind tunnel tests conducted on a Darrieus wind turbine. Journal of Wind Engineering and Industrial Aerodynamics 179:229–239. https://doi.org/10.1016/j.jweia.2018.06.002

Kedare S. B. , Date A. W. 1999. Performance characteristics of a reciprocating wind machine. J Wind Engineering and Industrial Aerodynamics 22(6):11-18. https://doi.org/10.1016/0167-6105(90)90147-5

Kumar A. 2017. Performance analysis of a Savonius hydrokinetic turbine having twisted blades. Renewable Energy Volume 113 :461-478. https://doi.org/10.1016/j.renene.2017.03.006

Marinic I., Vucina D. , Milas Z. 2019. Concept of flexible vertical-axis wind turbine with numerical simulation and shape optimization. Energy 167:841-852. https://doi.org/10.1016/j.energy.2018.11.026

Marinic I., Vucina D. , Milas Z. 2020. Computational analysis of Savonius wind turbine modifications including novel scooplet-based design attained via smart numerical optimization. Journal of Cleaner Production 262:121310. https://doi.org/10.1016/j.jclepro.2020.121310

Marmutova Svetlana. 2016. Performance of a Savonius wind turbine in urban sites using CFD analysis. Thesis, University of VAASA, Finland.

Mauro S., Brusca S., Lanzafame R., Messina M. 2019. CFD modeling of a ducted Savonius wind turbine for the evaluation of the blockage effects on rotor performance. Renewable Energy 141:28-39. https://doi.org/10.1016/j.renene.2019.03.125

Menet J. 2004. A double-step Savonius rotor for local production of electricity: a design study. Renewable Energy 29:1843–1862. https://doi.org/10.1016/j.renene.2004.02.011

Meziane M., Faqir M., Essadiqi E., Ghanameh M.F. 2020. CFD Analysis of the Effects of Multiple Semicircular Blades on Savonius Rotor Performance. I.J. Renewable Energy Research 10(3).

Mohamed H., Thevenin D. 2010. Performance optimization of a Savonius turbine considering different shapes for frontal guiding plates. In: Proceedings of the 10th international congress of fluid dynamics, 16-19 December, Egypt.

Mohamed M.H., Janiga G., Pap E., Thévenin D. 2010. Optimization of Savonius turbines using an obstacle shielding the returning blade. Renewable Energy 35:2618-2626. https://doi.org/10.1016/j.renene.2010.04.007

Mohammed H.A. 2013. Experimental comparison study for Savonius wind turbine of two & three blades at low wind speed. International Journal of Modern Engineering Research 3(5):2978-2986.

Mojica E.E, Fabay C.M, Kehinde F., Tenorio J.M. 2019. Design and development of integrated savonius and darrieus small scale vertical axis wind turbine for power generation. Earth and Environmental Science 291:012041. https://doi.org/10.1088/1755-1315/291/1/012041

Morcos S., Khalafallah M., Heikel H. 1981. The effect of sheilding on the aerodynamic performance of Savonius wind turbines. ASME 2:2037-2040.

Ogawa T., Yoshida H. 1986. The effect of deflecting plate and end plates on performance of savonius-type wind turbine. Bull. JSME 29(253).

Rezaeiha A., Montazeri H., Blocken B. 2019. On the accuracy of turbulence models for CFD simulations of verticalaxis wind turbines. Energy 180:838-857. https://doi.org/10.1016/j.energy.2019.05.053

Ross I., Altman A. 2011. Wind tunnel blockage corrections: Review and application to Savonius vertical-axis wind turbines. Journal of Wind Engineering and Industrial Aerodynamics. 99:523-538. https://doi.org/10.1016/j.jweia.2011.02.002

Roy S., Saha K. 2013. Review of experimental investigations into the design, performance and optimization of the Savonius rotor. J Power and Energy 227(4):528–542. https://doi.org/10.1177/0957650913480992

Roy S., Mukherjee P., Saha U. 2014. Aerodynamic performance evaluation of a novel Savonius-Style wind turbine under an oriented jet. In: Proceedings of the ASME 2014 Gas Turbine, India.

Roy S., Das R., Saha U.K. 2018. An inverse method for optimization of geometric parameters of a Savonius-style wind turbine. Energy Conversion and Management. 155:116-1127. http://dx.doi.org/10.1016/j.enconman.2017.10.0888

509 Saha U.K., Thotla S., Maity D. 2008. Optimum design configuration of Savonius rotor through wind
510 tunnel experiments. Journal of Wind Engineering and Industrial Aerodynamics 96:1359– 175.
511 https://doi.org/10.1016/j.jweia.2008.03.005
512 Shaheen M., El-Sayed, M., Abdallah S. 2015. Numerical study of two-bucket Savonius wind turbine
513 cluster. J. Wind Eng. Industrial Aerodyn. 137:78-89. https://doi.org/10.1016/j.jweia.2014.12.002
514 Shaughnessy B.M, Probert S.D. 1992. Partially-Blocked Savonius Rotor. Applied Energ. 43:239-249.
515 https://doi.org/10.1016/0306-2619(92)90024-6
516 Sobczak K. 2018. Numerical investigations of an influence of the aspect ratio on the Savonius rotor
517 performance. In: Conference series J. Physics. (1101)012034.
518 Tartuferi M., Alessandro V., Montelpare S., Ricci R. 2015. Enhancement of Savonius wind rotor
519 aerodynamic performance: a computational study of new blade shapes and curtain systems.
520 Energy 79:371-384. https://doi.org/10.1016/j.energy.2014.11.023
521 Wenehenubun F., Saputra A., Sutanto H. 2015. An experimental study on the performance of
522 Savonius wind turbines related with the number of blades. Energy Procedia 68:297-304.
523 https://doi.org/10.1016/j.egypro.2015.03.259
524 Yonghai H., Zhengmin T., Shanshan W. 2009. A new type of VAWT and blade optimization. In:
525 International Technology and Innovation Conference 2009 (ITIC 2009), China.
526 Zakaria A., Ibrahim M. 2020. Effect of twist angle on starting capability of a Savonius rotor – CFD
527 analysis. Materials Science and Engineering. 715:012014.